Journal of Materials and Electronic Devices 3 (2022) 20-26

Electrical Properties of InSe/PMItz Nanocomposite Thin Films

Fatih Ünal[1*], Merve Zurnacı[2], Serkan Demir[3], Mahmut Gür[4], Nesrin Şener[5], İzzet Şener[6]

[1] Central Research Laboratory, Application and Research Center, Giresun University, Giresun, Turkey
[2] Central Research Laboratory, Kastamonu University, Kastamonu, Turkey
[3] Department of Industrial Engineering, Faculty of Engineering, Giresun University, Giresun, Turkey.
[4] Department of Forest Industrial Engineering, Faculty of Forestry, Kastamonu University, Kastamonu, Turkey
[5] Chemistry Department, Faculty of Arts and Sciences, Kastamonu University, Kastamonu, Turkey
[6] Department of Food Engineering, Faculty of Engineering and Architecture, Kastamonu University, Kastamonu, Turkey

An outperforming inorganic semiconductor InSe thin films were growth on glass/ITO substrate by electrochemical deposition method and one group annealed. Organic semiconductor PMItz was successfully growth on two separate films by physical vapor deposition (PVD) method. For electrical analyses, heterojunctions were contacted with indium and their I-V characteristics were investigated under varying light intensities. From I-V measurements, it is calculated that ideality factors n were between 7.53-3.94 and 1.45-1.42, fill factors were between 0.25 and 0.26 and serial resistance Rs values were ≈$10^8\Omega$. It is observed from overall data that first time growth inorganic-organic heterojunctions herein exhibited photodiode and photovoltaic behaviours.

Keywords: *InSe; Organic semiconductor; hybrid heterojunction; photovoltaic cell; photodiode.*

Submission Date: 18 September 2022
Acceptance Date: 20 October 2022

**Corresponding author: fatih.unal@giresun.edu.tr*

1. Introduction

Outstanding optoelectronic properties of indium selenides (In_xSe_y) that can constitute varied elemental compositions still make them peculiar over the decades for the development of multivarious and functional electro-photonics [1-6]. Since their photodetective characteristics that outperform classical 2D semiconductors are promise for advanced data processing, storage and optical imaging technologies [7-12]. Their various and compatible heterojunctions with other III-VI semiconductors through Van der Waals epitaxy facilitate thermal and electrostatic tunability to achieve desired optical and electrical properties as well as to increase the diversity of the devices [13-17]. Dangling covalent bonds at their contact surfaces as their inherent property gives opportunity for easy heterointerface processing by reducing trap cites and ignoring lattice mismatch [18-20]. On the other hand, nonflexible film structure, relatively high production cost and paucity in variety of inorganic semiconductors are their major drawback for commercialization whereas small molecule-based organic semiconductors are more advantageous and have started to be more preferable in terms of their high abundance, relatively low fabrication costs, tunability of optoelectronic properties by chemical modification and more flexible film structure which also enables the design of biocompatible devices [21-25]. Therefore, studies based on organic semiconducting heterojunctions attract an increasing attention for last few decades. In connection with this, Phenanthrimidazoles as a popular class of π-conjugated organic semiconductors exhibit excellent photophysical and optoelectronic behaviours and are especially utilized for the fabrication of organic electroluminescent devices for a few decades [26-32]. But optoelectronics where phenanthroimidazoles were deposited on inorganic substrates are relatively rare. Also, organic-inorganic heterostructures where In_xSe_y were used as substrate were

not encountered in the literature so far to our knowledge. Moreover, heterojunction of organic and inorganic layers increases the variety of fabricated devices and eliminate the aforementioned drawbacks of inorganic semiconductors to some extent. In our previous study, we fabricated an ITO supported photodiode thin film of a newly synthesized phenanthroimidazole derivative (PMItz) which displays strong negative differential resistance (NDR) property both in the reverse and forward bias conditions[33]. As our ongoing research we herein deposited PMItz on In_xSe_y substrate by physical vapor deposition (PVD) method to fabricate a new organic-inorganic hybrid heterojunction. One of separately prepared two films was also annealed. Thus, it is aimed to take advantage of prominent electrical features of both In_xSe_y and PMItz. The obtained photodiode and photovoltaic behaviours of the first time fabricated InSe and PMItz based hybrid heterojunctions were observed.

2. Experimental

Autolab PGSTAT128N model electrochemical impedance spectroscopy instrument was used for electrochemical deposition. A Vaksis PVD-MT/2M2T thermal evaporation thin film deposition system was used for thermal deposition.

2.1. Construction of Glass/ITO/InSe thin films

In_xSe_y was growth on a glass/ITO substrate having specific resistance of lower than 20 Ω by electrochemical deposition method. The substrate was cleaned with deionized water, acetone, propanol and dried with nitrogen before deposition.

25 mM $InCl_3$ (sigma aldrich %99,999) for In source, 25 mM H_2O_3Se (sigma aldrich %98) for Se source, 250 mM LiCl (sigma aldrich %99) and 350 mM KCl (sigma aldrich %99) as buffer solutions were used. For one-step electrochemical deposition, electrolyte volume was set to 60 ml using 15 ml from each solution. The pH of the electrolyte was adjusted to 1,5 using 9,45 M HCl solution and applied voltage set to -0,95 V. Platin plate as counter electrode with the dimensions of 1,0 x 1,5 cm, Ag/AgCl reference electrode, and glass/ITO as working electrode with the surface area of 1 cm2 were used. The reaction was performed at room temperature during 60 min. and in nitrogen atmosphere with 0.1 bar. A set from obtained films was annealed at 70 cmHg and 105 ºC temperature during 60 min.

2.2. Fabrication of Glass/ITO/InSe/PMItz and Glass/ITO/InSe(annealed)/PMItz heterojunctions

PMItz as organic layer in powder form was growth on Glass/ITO/InSe and Glass/ITO/InSe(annealed) by using physical vapor deposition (PVD) method. The temperature and pressure of the chamber was set to 26 ºC and 10-6 torr respectively using Mo pot.

2.3. *Fabrication of In/InSe/PMItz/In and In/InSe(annealed)/In heterojunctions*

In metal contacts were coated on InSe, InSe(annealed) and Pmitz layers using the PVD method using a mask.

3. Results

3.1. Electrical Analyses

Fluctuations or changes in currents within heterojunctions by applied external potential are pivotal for electronic applications. Sometimes variations in measurements are possible by changing external parameters such as high-low temperature [34], exposition of heterojunction to incident light with different frequencies [35] or as in our study, varying of light intensity in constant frequency. Electrical analyses were performed in dark and 420 W/m^2 light intensity. The fabricated heterojunctions were contacted with indium by PVD as illustrated in Figure 1.

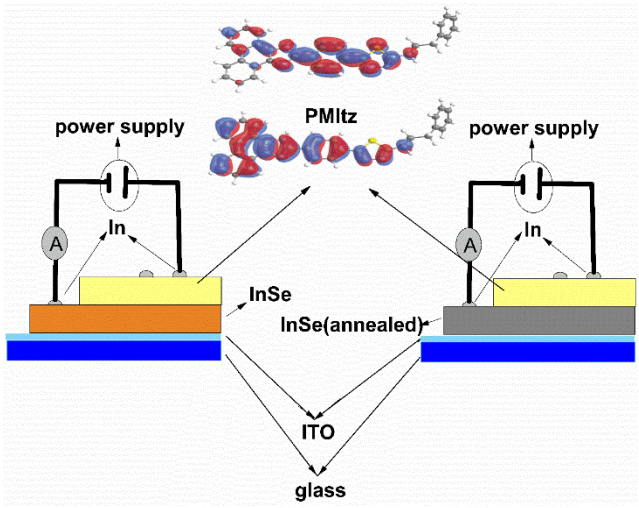

Figure 1. Schematic representation of In/InSe/PMItz/In(left) and In/InSe/PMItz(annealed)/In(right) devices.

In Figure 2a and 2b, ln(I) versus V graphs of In/InSe/PMItz/In and In/InSe/PMItz(annealed)/In devices in ±5 V range and under forward and reverse bias conditions at dark and illumination environment. The asymmetry of the plots in right and left parts is clearly seen. Unsaturated condition is observed in reverse bias, which originates from image force lowering of barrier height between PMItz layer and In contact [36-42]. This condition is more stable in In/InSe/PMItz(annealed)/In device. It is seen that the electrical conductivity of both heterojunctions increases in forward bias under light.

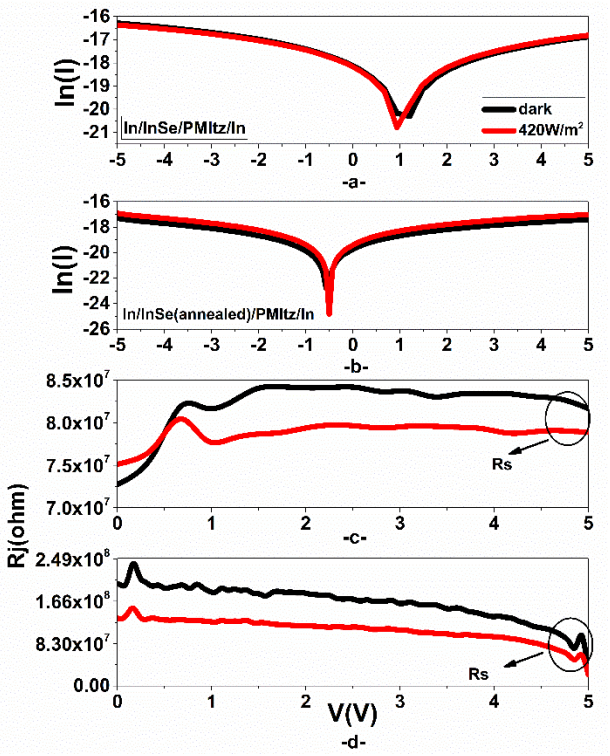

Figure 2. a) ln(I) versus. V, c) Rj versus. V plots of In/InSe/PMItz/In device and, b) ln(I) versus. V d) Rj versus V plots of In/InSe(annealed)/PMItz/In device in dark and 420W/m^2 light intensity condition.

In Figure 2c and 2d, Rj (junction resistance, Rj=dV/dI) versus V plots are given. Rj values of In/InSe/PMItz/In device changes between 8.5x10^{7}Ω and 7.2x10^{7}Ω while In/InSe/PMItz(annealed)/In device, Rj values are between 2.65x10^{8}Ω and 1.1x10^{8}Ω. Rj values of both heterojunction decreased with the light. Rs serial resistance can be also estimated from the above plot, where low Rs value indicates high current flow across the junction [43]. In heterojunctions under light, photons of higher energy than forbidden energy band gaps (Eg) generate new electron-hole pairs through depletion region. These pairs which make stress in the structure splits by strong internal electric field induced in particle boundaries. Electrons flow quickly through PMItz layer while holes are slower owing to trap levels. Accordingly, photoconductivity increased while Rj values decreased [36, 44].

Current-voltage relations of diodes (MIS, MPS, MOS, MS) are determined according to thermionic emission theory and diode parameters can be estimated by different methods [45-49], Norde method [50] and Cheung methods[51] are one of them. In our study, n and Rs values were calculated from the following equation which is the first one used in Cheung& Cheung method.

$$\frac{dV}{dln(I)} = IR_s + \frac{nkT}{q} \quad (9)$$

The slope of $\frac{dV}{dln(I)}$ versus I plot gives Rs values while n ideality factor is calculated from the y-intercept using other constants together [51].

The plot of $\frac{dV}{dln(I)}$ versus I, were given in Figure 3a-b for In/InSe/PMItz/In and In/InSe(annealed)/PMItz/In devices respectively. n values calculated from these curves are between 7.53 - 3.94 and 1.45 - 1.42 for In/InSe/PMItz/In and In/InSe(annealed)/PMItz/In devices respectively.

Although n values decreased with the light intensity, they are extremely far from unity, ideal diode value, especially for In/InSe/PMItz/In device. This arise from the existence interface states within PMItz layer, high density Nss values and barrier inhomogeneities[52]. Also the effects of image force effect, recombination and expansion of depletion region are possible.

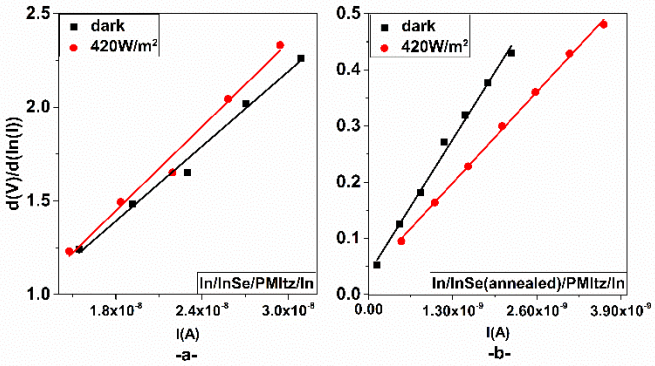

Figure 3 a) the plot of $\frac{dV}{dln(I)}$ versus I, of In/InSe/PMItz/In device and b) the plot of $\frac{dV}{dln(I)}$ versus I, of In/InSe/PMItz(annealed)/In device in dark and 420W/m2 light intensity condition.

Rs values of In/InSe/PMItz/In and In/InSe(annealed)/PMItz/In devices determined versus dark and light by different methods. Although there is not much change in In/InSe/PMItz/In with light, it is seen that there is a significant change in In/InSe(annealed)/PMItz/In. While Rs value from d(V)/d(ln(I)-I plot of In/InSe(annealed)/PMItz/In decreased from 1.83 x10^{8}Ω to 1.24x10^{8}Ω from dark to light, Rs value from Rj-V plot decreased from 1.26x10^{8}Ω to 7.38x10^{7}Ω from dark to light. Rs values calculated with different methods are in accordance with each other and behaviours against light are similar.

The fill factors (FF) were calculated from the formula $FF = \frac{Impp.Vmpp}{Isc.Voc}$ [53]. Where Isc is short circuit current, Voc is open circuit voltage, Impp is maximum power point current and Vmpp is maximum power point voltage values. In Figure 4a-b solar cell parameters of In/InSe/PMItz/In and In/InSe(annealed)/PMItz/In devices were given, respectively. The solar cell parameters of the devices were estimated from

the plots. It has been observed that both heterojunctions exhibit photodiode behaviour due to the change of Isc value under light. In addition, the FF value of the In/InSe(annealed)/PMItz/In device was higher than that of the In/InSe/PMItz/In device.

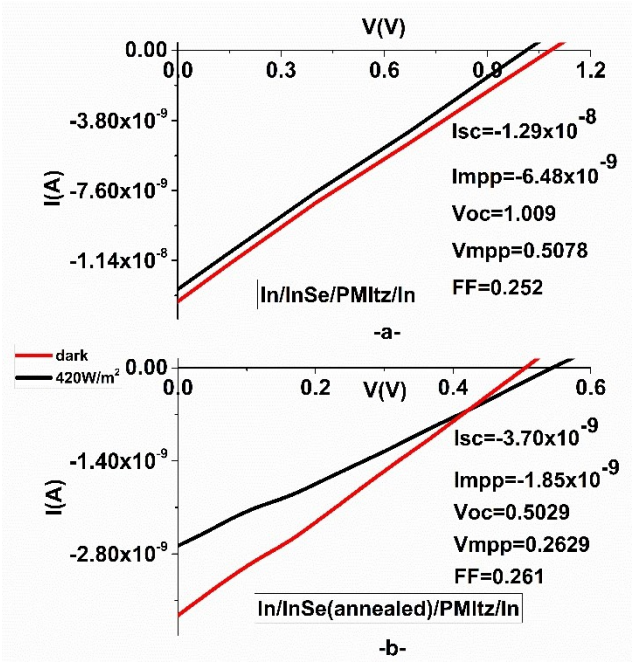

Figure 4. Solar cell parameters of a) In/InSe/PMItz/In and b) In/InSe(annealed)/PMItz/In devices.

Photocurrent (Iph=Iill-Idark), photoresponsivity (R=Iph/Pinc.A) and photosensitivity (S=R.T/V) are important parameters for diodes [54-60]. Where, Iill is the current in illuminated condition, Idark is the dark current, Pinc is the power of incident light (420W/m^2) and A is contact area(0.31x10^{-4}m^2) of diode, T is thickness of active layer (PMItz thicknes ≈ 6.12x10^{-7}m) and V is applied bias voltage. In Figure 5, the variation of a) Iph, b) R and c) S values versus different voltage values of devices under forward bias and in 420 W/m^2 light intensity is given. The Iph, R and S values of the In/InSe/PMItz/In device are 9.74x10^{-10} – 3.47x10-9 A, 7.38x10^{-8} - 2.63x10^{-7}(A/W), 4.43x10^{-14} - 3.16x10^{-14} S.m/W, respectively. The Iph, R and S values of the In/InSe(annealed)/PMItz/In device are 3.75x10^{-9} - 1.36x10-8 A, 2.84x10^{-7} - 1.03x10^{-6} (A/W), 1.70x10^{-13} - 1.23x10^{-13} S.m/W, respectively. It is seen that Iph, R and S values of In/InSe(annealed)/PMItz/In device are higher than these of In/InSe/PMItz/In device at all voltage values. It is found that In/InSe(annealed)/PMItz/In device is a better diode than In/InSe/PMItz/In device. Annealing of the InSe layer improved the optical properties of the device as well as its electrical properties.

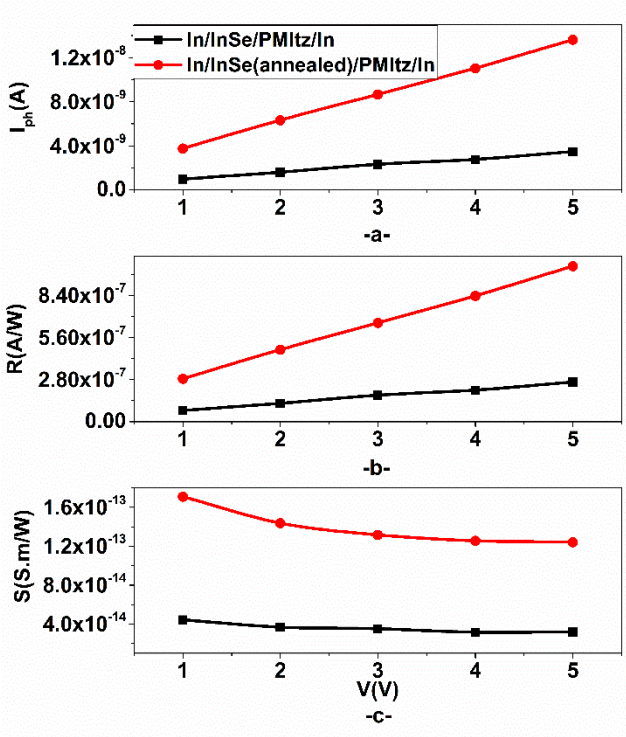

Figure 5. the variation of a) Iph, b) R and c) S values versus different voltage values of devices under forward bias and in 420 W/m2 light intensity

4. Conclusion

InSe thin films were obtained successfully on to glass/ITO substrate by electrochemical deposition method. Organic PMItz semiconductor was deposited on the obtained thin films by PVD method. Indium contacts were jointed heterojunctions and electrical parameters were investigated under dark and 420W/m^2 light intensity. It is concluded that heterojunctions are light sensitive, power generation take places in photovoltaic region and they act as photodiode under reverse bias conditions.

References

1. Camara, M.O.D., A. Mauger, and I. Devos, Electronic structure of the GaSe/Si(111) and InSe/Si(111) heterojunctions. Physical Review B, 2002. **65**(20).

2. Camara, M.O.D., A. Mauger, and I. Devos, Electronic structure of the layer compounds GaSe and InSe in a tight-binding approach. Physical Review B, 2002. **65**(12).

3. Gopal, S., et al., Conduction studies on electrodeposited indium selenide thin films. Ionics, 2004. **10**(3-4): p. 300-303.

4. Igasaki, Y. and T. Fujiwara, The preparation of highly oriented InSe films by electrodeposition.

Journal of Crystal Growth, 1996. **158**(3): p. 268-275.

5. Fadel, M., et al., Structural and optical properties of SeGe and SeGeX (X=In, Sb and Bi) amorphous films. Journal of Alloys and Compounds, 2009. **485**(1): p. 604-609.

6. Ma, Y.D., et al., Engineering a topological phase transition in beta-InSe via strain. New Journal of Physics, 2013. **15**.

7. Mudd, G.W., et al., Tuning the Bandgap of Exfoliated InSe Nanosheets by Quantum Confinement. Advanced Materials, 2013. **25**(40): p. 5714-+.

8. Han, G., et al., Indium Selenides: Structural Characteristics, Synthesis and Their Thermoelectric Performances. Small, 2014. **10**(14): p. 2747-2765.

9. Yuksek, M., et al., Nonlinear and saturable absorption characteristics of Ho doped InSe crystals. Optics Communications, 2014. **310**: p. 100-103.

10. Ho, C.H. and Y.J. Chu, Bending Photoluminescence and Surface Photovoltaic Effect on Multilayer InSe 2D Microplate Crystals. Advanced Optical Materials, 2015. **3**(12): p. 1750-1758.

11. Politano, A., et al., Indium selenide: an insight into electronic band structure and surface excitations. Scientific Reports, 2017. **7**.

12. Zhou, J.D., et al., InSe monolayer: synthesis, structure and ultra-high second-harmonic generation. 2d Materials, 2018. **5**(2).

13. Sen, S.S., N.N. Biswas, and K.A. Khan, Temperature effect on the electrical and optical properties of indium-selenide thin-films. Applied Energy, 2000. **65**(1-4): p. 51-58.

14. Bouzouita, H., et al., Preparation and characterization of In2Se3 thin films. Renewable Energy, 2002. **25**(1): p. 131-138.

15. El-Sayed, S.M., Optical investigations of the indium selenide glasses. Vacuum, 2003. **72**(2): p. 169-175.

16. Pathan, H.M., et al., Preparation and characterization of indium selenide thin films from a chemical route. Materials Chemistry and Physics, 2005. **93**(1): p. 16-20.

17. Ornelas, R.E., et al., In6Se7 thin films by heating thermally evaporated indium and chemical bath deposited selenium multilayers. Applied Surface Science, 2012. **258**(15): p. 5753-5758.

18. Wang, Y., et al., Molecular Doping of 2D Indium Selenide for Ultrahigh Performance and Low-Power Consumption Broadband Photodetectors. Advanced Functional Materials, 2021. **31**(30).

19. Sanchez-Royo, J.F., et al., Electronic structure, optical properties, and lattice dynamics in atomically thin indium selenide flakes. Nano Research, 2014. **7**(10): p. 1556-1568.

20. Cho, S.H., et al., Bias-controlled multi-functional transport properties of InSe/BP van der Waals heterostructures. Scientific Reports, 2021. **11**(1).

21. Zhou, Y., Optoelectronic Organic–Inorganic Semiconductor Heterojunctions. 1st ed, ed. Y. Zhou. 2021: CRC Press. 351.

22. Wang, Z., L. Huang, and L. Chi, Organic Semiconductor Field-Effect Transistors Based on Organic-2D Heterostructures. Frontiers in Materials, 2020. **7**(295).

23. Novota, M., et al., New phenanthrene-based organic semiconductor material for electronic devices. 2014 10th International Conference on Advanced Semiconductor Devices & Microsystems (Asdam), 2014: p. 97-100.

24. Pudasaini, P.R. and A.A. Ayon, Low-cost, high-efficiency organic/inorganic hetero-junction hybrid solar cells for next generation photovoltaic device. 13th International Conference on Micro and Nanotechnology for Power Generation and Energy Conversion Applications (Powermems 2013), 2013. **476**.

25. Li, G.W., et al., Planar Conjugated Polymers Containing 9,10-Disubstituted Phenanthrene Units for Efficient Polymer Solar Cells. Macromolecular Rapid Communications, 2014. **35**(12): p. 1142-1147.

26. Jayabharathi, J., P. Ramanathan, and V. Thanikachalam, Synthesis and optical properties of phenanthromidazole derivatives for organic electroluminescent devices. New Journal of Chemistry, 2015. **39**(1): p. 142-154.

27. Zhuang, S.Q., et al., Efficient nondoped blue organic light-emitting diodes based on phenanthroimidazole-substituted anthracene derivatives. Organic Electronics, 2012. **13**(12): p. 3050-3059.

28. Sun, Y.F., et al., The synthesis, two-photon absorption and blue upconversion fluorescence of novel, nitrogen-containing heterocyclic

chromophores. Dyes and Pigments, 2009. **81**(1): p. 10-17.

29. Wang, B., et al., Pyridine-containing phenanthroimidazole electron-transport materials with electron mobility/energy-level trade-off optimization for highly efficient and low roll-off sky blue fluorescent OLEDs. Journal of Materials Chemistry C, 2015. **3**(29): p. 7709-7719.

30. Chen, W.C., et al., Molecular modification on bisphenanthroimidazole derivative for deep-blue organic electroluminescent material with ambipolar property and high performance. Organic Electronics, 2015. **17**: p. 159-166.

31. Li, C.L., et al., High performance full color OLEDs based on a class of molecules with dual carrier transport channels and small singlet-triplet splitting. Chemical Communications, 2015. **51**(53): p. 10632-10635.

32. Wang, Z.M., et al., Phenanthro[9,10-d]imidazole as a new building block for blue light emitting materials. Journal of Materials Chemistry, 2011. **21**(14): p. 5451-5456.

33. Zurnaci, M., et al., Synthesis of a new 1,3,4-thiadiazole-substituted phenanthroimidazole derivative, its growth on glass/ITO as a thin film and analysis of some surface and optoelectronic properties. New Journal of Chemistry, 2021. **45**(48): p. 22678-22690.

34. Kumar, A., et al., Structural and Electrical Properties of Ag/n-TiO2/p-Si/Al Heterostructure Fabricated by Pulsed Laser Deposition Technique. Journal of Electronic Materials, 2017. **46**(11): p. 6422-6429.

35. Basir, A., et al., A novel self-powered photodiode based on solution-processed organic TPD:Alq3 active layer. Materials Science in Semiconductor Processing, 2021. **131**: p. 105886.

36. Rhoderick, E.H.W.R.H., Metal-semiconductor contacts. 1988, Oxford [England]; New York: Clarendon Press ; Oxford University Press.

37. Reddy, P.R.S., et al., Modification of Schottky Barrier Properties of Ti/p-type InP Schottky Diode by Polyaniline (PANI) Organic Interlayer. Journal of Semiconductor Technology and Science, 2016. **16**(5): p. 664-674.

38. Dobrescu, D., et al., Image force effect on forward characteristic of a rectifier metal-semiconductor contact. 2001 International Semiconductor Conference, Vol 1 & 2, Proceedings, 2001: p. 429-432.

39. Aktas, S., Electrical characterisation of photosensitive Si/W–Ge oxide composite heterojunction. Optical Materials, 2022. **132**: p. 112839.

40. Unal, F., M.S. Kurt, and S. Durdu, Investigation of the effect of light on the electrical parameters of Si/TiO2 heterojunctions produced by anodic oxidation on p-type Si wafer. Journal of Materials Science: Materials in Electronics, 2022.

41. AktaŞ, S. and F. ÜNal, Investigation of Structural and Electrical Properties of Metal Oxide and Organic Based Multi Heterojunction. Karadeniz Fen Bilimleri Dergisi, 2022. **12**(1): p. 508-520.

42. ÜNal, F. and S. AktaŞ, Electrical Characterization of n-type doped metal oxide/p-type Si Photosensitive Heterojunction. Journal of the Institute of Science and Technology, 2022: p. 1506-1517.

43. Reddy, V.R., et al., Electrical and carrier transport properties of Ti/alpha-amylase/p-InP MPS junction with a alpha-amylase polymer interlayer. Journal of Materials Science-Materials in Electronics, 2021. **32**(6): p. 8092-8105.

44. Çetinkaya, H.G., et al., Photovoltaic characteristics of Au/PVA (Bi-doped)/n-Si Schottky barrier diodes (SBDs) at various temperatures. Current Applied Physics, 2013. **13**(6): p. 1150-1156.

45. Al-Ta'ii, H.M.J., V. Periasamy, and Y.M. Amin, Electronic Characterization of Au/DNA/ITO Metal-Semiconductor-Metal Diode and Its Application as a Radiation Sensor. Plos One, 2016. **11**(1).

46. Yakuphanoglu, F., Photovoltaic properties of the organic-inorganic photodiode based on polymer and fullerene blend for optical sensors. Sensors and Actuators a-Physical, 2008. **141**(2): p. 383-389.

47. Aslan, N., et al., Ti doped amorphous carbon (Al/Ti-a:C/p-Si/Al) photodiodes for optoelectronic applications. Journal of Molecular Structure, 2018. **1155**: p. 813-818.

48. Aslan, N., et al., Ti doped amorphous carbon (Al/Ti-a: C/p-Si/Al) photodiodes for optoelectronic applications. Journal of Molecular Structure, 2018. **1155**: p. 813-818.

49. Koç, M.M., et al., Electrical characterization of solar sensitive zinc oxide doped-amorphous carbon photodiode. Optik, 2019. **178**: p. 316-326.

50. Norde, H., A modified forward I-V plot for Schottky diodes with high series resistance. Journal of Applied Physics, 1979. **50**(7): p. 5052-5053.

51. Cheung, S.K. and N.W. Cheung, Extraction of Schottky Diode Parameters from Forward Current-Voltage Characteristics. Applied Physics Letters, 1986. **49**(2): p. 85-87.

52. Arslan, E., et al., Tunneling current via dislocations in Schottky diodes on AlInN/AlN/GaN heterostructures. Semiconductor Science and Technology, 2009. **24**(7): p. 075003.

53. Ünal, F., Investigation of Diode Parameters of Photoconductive and Photovoltaic p-Type Si/Ge-Doped WOx Heterojunction. Journal of Electronic Materials, 2022.

54. Gündüz, B., et al., The photo-electrical properties of the p-Si/Fe(II)–polymeric complex/Au diode. Synthetic Metals, 2013. **184**: p. 73-82.

55. Zhang, X., et al., ZnSe nanowire/Si p-n heterojunctions: Device construction and optoelectronic applications. Nanotechnology, 2013. **24**(39).

56. Patel, A., et al., Fabrication, photoresponse and temperature dependence of n-VO2/n-MoSe2 heterojunction diode. Superlattices and Microstructures, 2019. **130**: p. 160-167.

57. Sarcan, F., ZnO nanoparticles-based vacuum pressure sensor. Nanotechnology, 2020. **31**(43): p. 435502.

58. Sarcan, F., et al., Ultraviolet Photodetector Based on Mg0.67Ni0.33O Thin Film on SrTiO3. physica status solidi (RRL) – Rapid Research Letters, 2020. **14**(8): p. 2000175.

59. Sarcan, F., et al., A study on the voltage-dependent response of a GaInNAs-based pin photodetector with a quasi-cavity. Semiconductor Science and Technology, 2018. **33**(11): p. 114006.

60. Doğan, Ü., et al., Effects of annealing temperature on a ZnO thin film-based ultraviolet photodetector. Physica Scripta, 2022. **97**(1): p. 015803.